ADVANCES IN ATMOSPHERIC SCIENCES, VOL. 25, NO. 6, 2008, 1085–1097

Simulation and Analysis of China Climate Using Two-Way Interactive Atmosphere-Vegetation Model (RIEMS-AVIM)

GAO Rong*[1,4] (高 荣), DONG Wenjie[2] (董文杰), and WEI Zhigang[3] (韦志刚)

[1] *Laboratory of Climate Studies, National Climate Center, China Meteorological Administration, Beijing* 100081

[2] *State Key Laboratory of Earth Surface Processes and Ecology Resource, Beijing Normal University, Beijing* 100875

[3] *Cold and Arid Regions Environmental and Engineering Research Institute, Chinese Academy of Sciences, Lanzhou* 730000

[4] *Key Laboratory of Regional Climate-Environment for East Asia, Institute of Atmospheric Physics, Chinese Academy of Sciences, Beijing* 100029

(Received 29 December 2007; revised 7 April 2008)

ABSTRACT

In this paper, an Atmosphere-Vegetation Interaction Model (AVIM) is coupled to the Regional Integrated Environment Model System (RIEMS), and a 10-year integration for China is performed using the RIEMS-AVIM. The analysis of the results of the 10-year integration shows that the characters of the spatial distributions of temperature and precipitation over China are well simulated. The patterns of simulated surface sensible and latent heat fluxes match well with the spatial climatological atlas: the values of winter surface sensible and latent heat fluxes are both lower than climatological values over the whole country. Summer surface sensible heat flux is higher than climatological values in western China and lower in eastern China, while summer surface latent heat flux is higher than climatological values in the eastern and lower in the western. Seasonal variations of simulated temperature and precipitation of RIMES-AVIM agree with those of the observed. Simulated temperature is lower than the observed in the Tibetan Plateau and Northwest China for the whole year, slightly lower in the remaining regions in winter, but consistent with the observed in summer. The simulated temperature of RIEMS-AVIM is higher in winter and lower in summer than that of RIEMS, which shows that the simulated temperature of RIEMS-AVIM is closer to the observed value. Simulated precipitation is excessive in the first half of the year, but consistent with the observed in the second half of the year. The simulated summer precipitation of RIEMS-AVIM has significant improvement compared to that of RIEMS, which is less and closer to the observed value. The interannual variations of temperature and precipitation are also fairly well simulated, with temperature simulation being superior to precipitation simulation. The interannual variation of simulated temperature is significantly correlated with the observed in Northeast China, the Transition Region, South China, and the Tibetan Plateau, but the correlation between precipitation simulation and observation is only significant in Northwest China.

Key words: vegetation, regional model, two-way coupling, numerical simulation

Citation: Gao, R., W. J. Dong, and Z. G. Wei, 2008: Simulation and analysis of China climate using two-way interactive atmosphere-vegetation model (RIEMS-AVIM). *Adv. Atmos. Sci.*, **25**(6), 1085–1097, doi: 10.1007/s00376-008-1085-2.

1. Introduction

The feedback of variations in vegetation cover to climate change is an important topic in global change study, and the environmental and climatic effects of vegetation variations are listed as one of the key items in the International Geosphere-Biosphere Programme (IGBP), World Climate Research Programme (WCRP), International Human Dimensions Programme (IHDP) international research programs.

*Corresponding author: GAO Rong, gaor@cma.gov.cn

In the climate system, climate and vegetation are in a dynamical equilibrium, once they become out of balance due to changes in any one of two parties, a longer period of time is needed to reestablish a new equilibrium. Variation in vegetation cover exerts an influence on climate change by altering the exchanges of energy, moisture, and momentum between land and atmosphere, while variations in vegetation itself are affected by solar radiation, temperature. precipitation and other climatic factors (Nemani et al., 2003).

Currently, the expression of vegetation in most climate models is static, i.e., a prescribed annual cycle is used, and no interannual variation in vegetation is considered. Obviously, a long time integration of such a model is not able to actually describe the influence of vegetation change on climate and its response to climate. Foley et al. (1998) coupled the dynamic global vegetation model Integrated Biosphere Simulator version 1 (IBIS1) to a GCM model (GENESIS2, Global Environmental and Ecological Simulation of Interactive System version 2), and found that the coupled GENESIS-IBIS model is able to correctly simulate the belt-like distributions of temperature and precipitation and better simulate the positions of forests and grasses. Zeng et al. (1999) incorporated a dynamic relation of precipitation and leaf-area index (LAI) into a simple coupled Quasi-Equilibrium Tropical Circulation Model (QTCM) to simulate Sahel precipitation, and discovered that the coupled model is able to better simulate the interannual and interdecadal variations of precipitation in the Sahel region than the QTCM model itself. Cox et al. (2000) coupled a dynamic vegetation model TRIFFID (Terrestrial Representation of Interactive Foliage and Flora Including Dynamics) to the HadCM3, and found that the global warming effect in the coupled model is even stronger than that in the HadCM3, in which there is no carbon cycle considered. Snyder et al. (2004) coupled the dynamic global vegetation model IBIS1 to the general circulation model CCM3 and explored the feedback of changes in vegetation to regional precipitation. Dan et al. (2005) incorporated the land surface model Atmosphere-Vegetation Interaction Model to the Global Ocean-Atmosphere-Land System (GOALS), and found that the coupled model is able to better simulate the distributions of global climate and biomass and their evolution.

As for regional climate models, Tsvetsinskaya et al. (2001) incorporated the crop growth process into the BATS (Biosphere-Atmosphere Transfer Scheme), which was then coupled to the NCAR Regional Spectral Model (RSM) to simulate the influences of the seasonal variations of vegetation growth on exchanges of heat, moisture and momentum between land and atmosphere, and discovered that the coupled model reconciled the gap between the simulation and the observed in comparison with the NCAR RSM without incorporating the vegetation growth processes. The coupling of the crop growth model SUCROS (Simple and Universal Crop growth Simulator) and the RegCM3 (Regional Climate Model of the third generation) by Song et al. (2003) improved the simulation of summer temperature and precipitation over eastern China. Lu et al. (2001) coupled the ecosystem system model CENTURY to the regional atmospheric model RAMS (Regional Atmosphere Modeling System), and simulated the bioprocess on the timescale of one week in the central U.S.A. Chen and Pollarid (2004) and Chen et al. (2004) coupled the BIOME3 (the third generation of BIOgenic Model for Emissions) to the CMM5 (the fifth-generation of PSU/NCAR Mesoscale Model-based regional Climate model), and found from the East Asian climate simulation that when the CO_2 concentration is doubled, the climate will become warmer/drier in northern China, and warmer/wetter in the region south of the Huaihe River. The maximum temperature increase might reach 4°C in northern China, causing the degradation of natural vegetation. The strongest response of the vegetation to the climate change suggests that northern China is a sensitive area for climate-vegetation interaction. Zhang (2005) incorporated a dynamic relation between temperature and leaf-area index into the SNURCM (Seoul National University Regional Climate Model), and found that vegetation-atmosphere interaction can reduce the simulation error of climate in the surface layer.

Global models are frequently not able to simulate detailed regional climate changes due to their lower resolutions, and as for regional models, some regional models only contain the interaction between the atmosphere and one kind of vegetation. Other regional models incorporate some empirical interaction relations, but do not include the complete process of atmosphere-vegetation interaction. Therefore, this paper couples the atmosphere-vegetation interaction model AVIM to a regional climate model (Regional Integrated Environmental Model System) to simulate the regional climate characteristics in China, as well as to test the climate simulation ability of the RIEMS-AVIM for the purpose of further improvement of the model.

2. Brief introduction of the model and the design of interface

The Key Laboratory of Regional Climate-Environment for Temperate East Asia (RCE-TEA),

CAS, developed the Regional Integrated Environmental Model System (RIEMS) in 1998 (Fu et al., 2000), which takes the PSU/NCAR MM5(V2) as the dynamic framework and incorporates the physical process schemes necessary for climate research (mainly including the revised CCM3 radiation scheme and the BATS1e), and therefore is able to consider impact of vegetation on the atmosphere, not two-way coupling. The RIEMS had a better performance in the first and second phases of RMIP (Regional Climate Model Inter-comparison Project) (Fu et al., 2005; Feng, 2006).

The AVIM was developed by Ji (1995) from his simplified one dimensional Land surface Process Model (LPM; Ji and Hu, 1989) incorporating a vegetation physiology module, which includes one physical process module and one biological process module (Fig. 1). The major characteristic of AVIM is that vegetation parameters such as LAI and NPP are not prescribed, but computed from a dynamic vegetation module. In the new model, the RIEMS atmospheric mode, at first, transfers climatic variables such as temperature, precipitation, wind speed, humidity, surface pressure, and downward longwave and solar radiation to the land surface model (AVIM), then the AVIM returns sensible heat flux, latent heat flux, surface drag coefficient, and land surface albedo to the RIEMS after computation. The vegetation type is constant in AVIM, but the biomass including LAI and NPP is variable with the climate change. In the EMDI (Ecosystem Model-Data Intercomparison) activity, the AVIM was one of the best models whose NPP simulation value is closest to the observed value (11 models in all, see http://gaim.unh.edu/Structure/Intercomparison/EMDI/)

Exchanges between the atmosphere and land surface are realized mainly through the vertical diffusion items in the atmospheric equation group, expressed as

$$(F_{\rm v}\boldsymbol{V}, F_{\rm v}T, F_{\rm v}M) = \frac{g}{p^*}\frac{\partial}{\partial\sigma}\{\boldsymbol{\tau}\boldsymbol{V}, H/c_p, E\}\ ,$$

$$\boldsymbol{\tau} = \rho C_D \mid \boldsymbol{V}_{\rm a} \mid\ ,$$

$$H = H_{\rm a} = \rho c_p(T_{\rm af} - T_{\rm a})/r_{\rm a}\ ,$$

$$E = E_{\rm a} = \rho(q_{\rm af} - q_{\rm a})/r_{\rm a}\ ,$$

where the subscript v donotes the vertical direction, thus $F_{\rm v}\boldsymbol{V}, F_{\rm v}T, F_{\rm v}M$ are vertical momentum, heat and water vapor fluxes respectively. $\boldsymbol{V}, T_{\rm a}, q_{\rm a}$ are air velocity, potential temperature, and specific humidity in the lowest layer of the atmospheric model. $T_{\rm af}, q_{\rm af}, r_{\rm a}$ are air potential temperature, specific humidity and aerodynamical resistance within the canopy, respectively, which are complex functions of LAI and calculated by AVIM. ρ, c_p, C_D are air density, specific heat at constant pressure and drag coefficient influenced by LAI, and $\boldsymbol{\tau}, H, E$ are transfers of momentum, heat and water vapor fluxes between air and land. p^* and g are the depth of the lowest layer of atmosphere and acceleration of gravity.

The two-way coupling of AVIM and RIEMS is implemented by replacing the land surface process model originally embedded in the RIEMS with the AVIM, and is illustrated in Fig. 2. In the two-way coupling process, there is an interactive impact between atmosphere and vegetation. When the climate changes, the vegetation will follow, and then the climate also changes with the variation in vegetation.

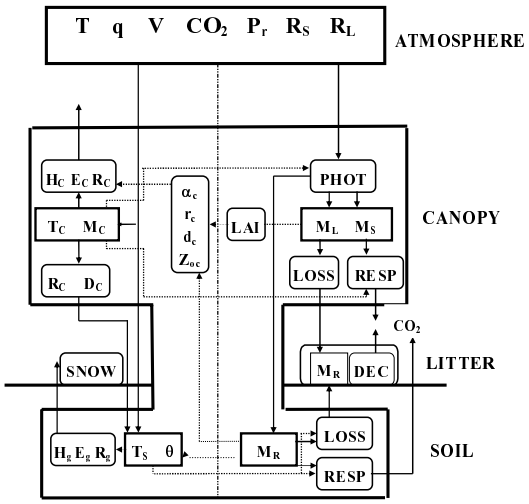

Fig. 1. Schematic structure of the atmosphere-vegetation interaction model (AVIM). The physical processes are displayed on the left side and biological processes on the right side (Ji, 1995).

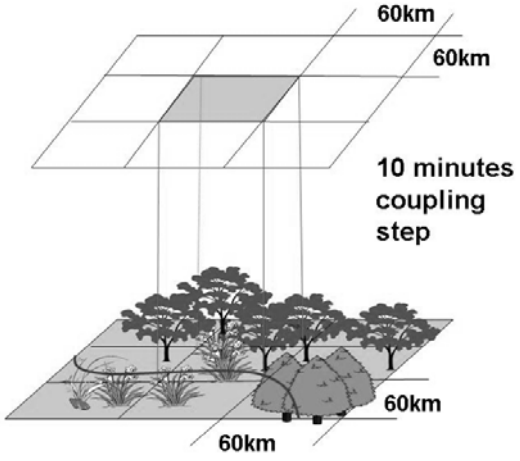

Fig. 2. Schematic diagram for coupling of AVIM and RIEMS.

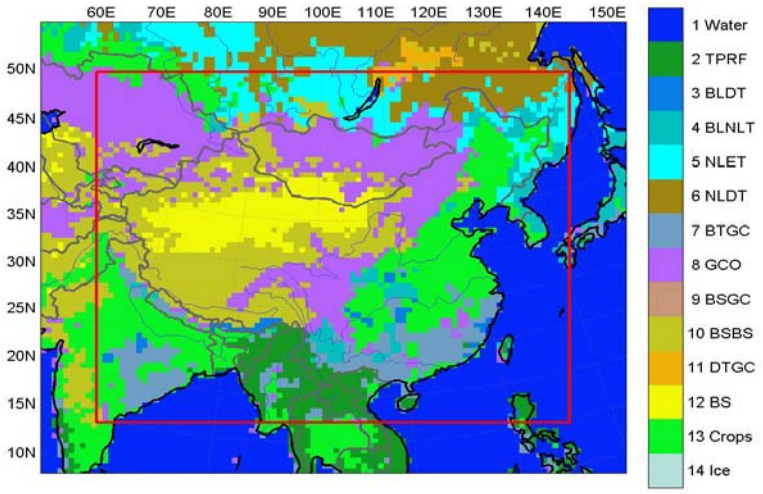

Fig. 3. Study area and vegetation distribution (1 Water; 2 Tropical rainforest; 3 Broadleaf deciduous trees; 4 Broadleaf and needle leaf trees; 5 Needle leaf evergreen trees; 6 Needle leaf deciduous trees; 7 Broadleaf trees with ground cover; 8 Ground cover only; 9 Broadleaf shrub with ground cover; 10 Broadleaf shrubs with bare soil; 11 Dwarf trees with ground cover; 12 Bare soil; 13 Crops; 14 Ice).

3. Simulation of climatic mean fields

To test the simulation ability of the RIEMS coupled with the AVIM (RIEMS-AVIM), the study area was taken as a rectangle with its center at (37°N, 102°E) and the horizontal resolution being 60 km, totaling 105×91 grid cells (Fig. 3), which contained a outer buffer region (10 grids in width) departing far away from the Tibetan Plateau (an area with larger computational errors). Also there is an inner region covering the whole China mainland (the red line rectangular in Fig. 3). The model was driven by the NCEP2 reanalysis data at a spatial resolution of 2.5° × 2.5° and a time resolution of 4 times per day, and has run for more than 10 years from 0000 UTC 1st July 1988 to 1800 UTC 31st December 1998. Among the results only the latter 10 years were used in analysis. Used in the computation of physical processes of the model were the following: the index relaxation boundary condition, Holtslag's planetary boundary-layer scheme, a simple ice phase explicit moisture scheme, the Grell cumulus convection parameterization scheme, AVIM land process, and revised CCM3 radiation scheme.

Figure 4 and 5 give the winter and summer average temperatures observed at 740 stations in China and simulated by the RIEMS and RIEMS-AVIM model, respectively. It can be seen from Fig. 4a that winter isotherms are parallel to latitude lines in eastern China, but consistent with topographic contours in the western China. The RIEMS and RIEMS-AVIM model are both able to well simulate the above pattern of winter temperatures, however the values of simulated temperatures are slightly lower than the observed in most areas in China (Fig. 4b and Fig. 4c). The contour of observed 0°C temperature goes from the lower reach of the Yellow River westwards to the Shaanxi Plain, then turns southwestwards along the east fringe of the Tibetan Plateau. However, the simulated 0°C contours both lie south of the observed in eastern China, they go from the lower reach of the Huaihe River west-southwest-wards to the middle reaches of the Yangtze River. It then moves around the NW edge of the Sichuan Basin, and at last turns west-southwest-wards along the SE fringe of the Tibetan Plateau. The simulated winter temperature is almost identical to the observed in the Tarimu Basin and the northern parts of Northeast China, but lower in the western Tibet Plateau and extreme Southern China. This might be caused by the oversimulated winter Mongolia high (Figure not shown), which brings about intense winter monsoon to South China. The simulated temperature of RIEMS-AVIM is almost identical with that of RIEMS in South China, but it's higher than that of RIEMS in western China, North China and Northeast China. In summer, the western Pacific subtropical high extends westwards as well as moves northwards, and temperature is high over most areas in China except the Tibetan Plateau, in particular, in the area south of the Yellow River in eastern China where the mean temperature is greater than 24°C (Fig. 5a). The RIEMS and RIEMS-AVIM simulated summer tem-

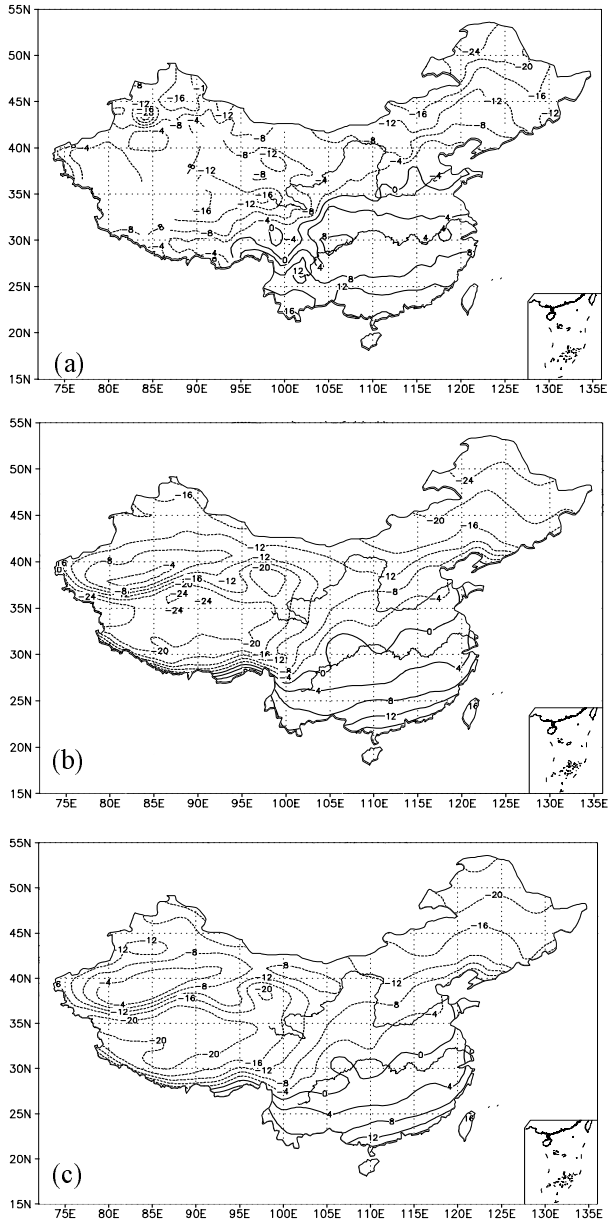

Fig. 4. (a) Observed, (b) RIEMS and (c) RIMS-AVIM simulated winter mean temperature over China (units: °C).

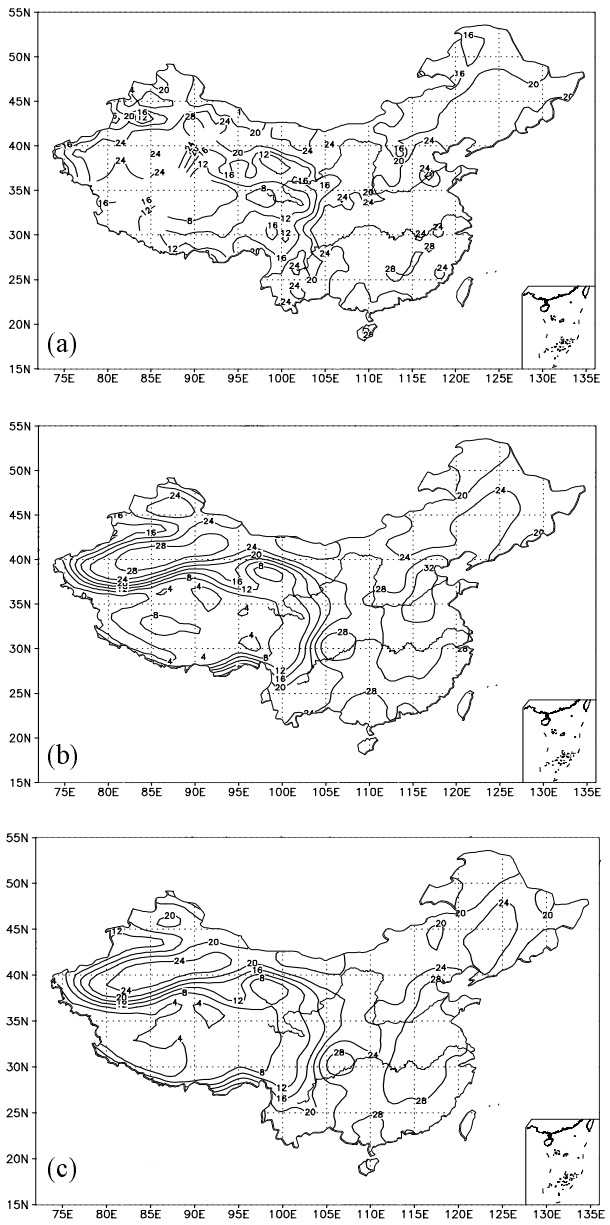

Fig. 5. (a) Observed, (b) RIEMS and (c) RIEMS-AVIM simulated summer mean temperatures over China (units: °C).

perature is basically in accord with the observed, with the high temperature centers in the Tarimu Basin and western Inner Mongolia being well simulated. The simulated temperature of RIEMS-AVIM is lower than that of RIEMS and is closer to the observed in most of China, and the RIEMS-AVIM has improved the simulated ability for summer temperatures (Fig. 5b and Fig. 5c). The simulation errors of summer temperature might mainly originate from the deviations of simulated atmosphere circulation and land and air exchanges in comparison with the observed values.

Precipitation simulation, especially in summer, has been an emphasis and difficulty for a long time in developing climate models. Figures 6 and 7 exhibit the observed, RIEMS and RIEMS-AVIM simulated daily precipitation for winter and summer, respectively. In winter, China is dominantly influenced by the Mongolia high, or winter monsoon, and precipitation is sparse in most areas except in the vicinity of Nanling Mountains where rainfall is greater than 3 mm d^{-1} (Fig. 6a). The RIEMS and RIEMS-AVIM simulated winter precipitation is basically in agreement with the observed.

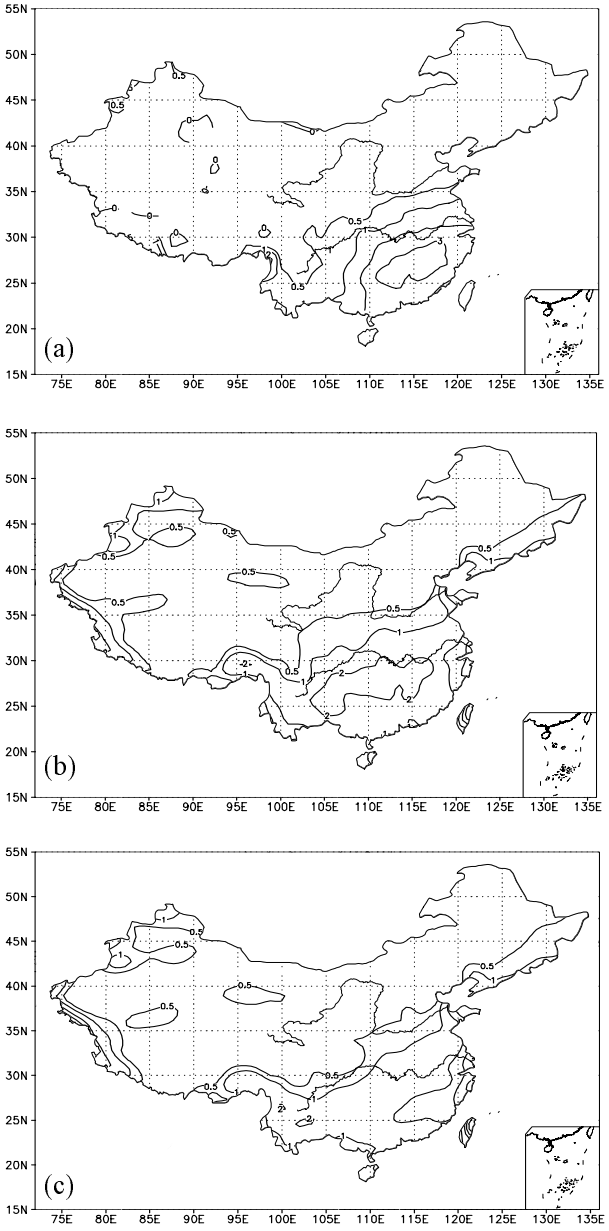

Fig. 6. (a) Observed, (b) RIEMS and (c) RIEMS-AVIM simulated winter mean daily rainfall over China (units: mm d^{-1}).

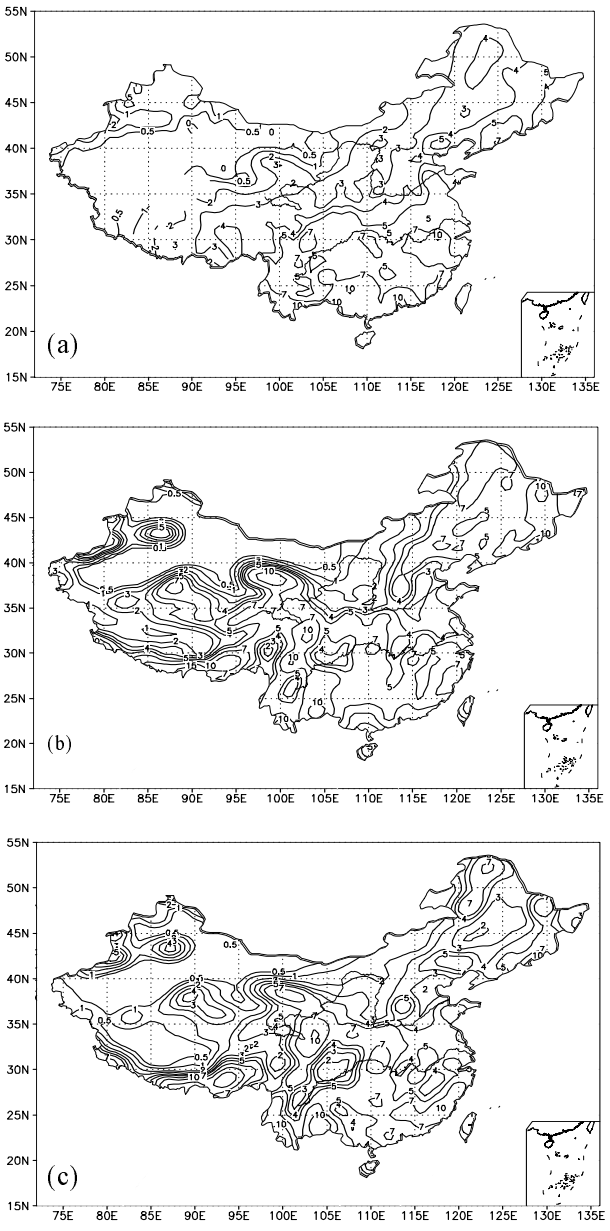

Fig. 7. (a) Observed, (b) RIEMS and (c) RIEMS-AVIM simulated winter mean daily rainfall over China (units: mm d^{-1}).

The simulated precipitation is sparse in most areas in China, and the area with a daily rainfall greater than 1 mm d^{-1} is larger than the observed but the area with greater than 2 mm d^{-1} is smaller with its location south of the observed (Figs. 6b and 6c). In summer, the Indian summer monsoon and South China Sea summer monsoon transfer abundant moisture towards China, thus, precipitation is greater in most areas in China. The isoline of daily rainfall of 3 mm d^{-1} extends from the Daxinganling Mountains to the Taihang Mountains, and then successively crosses the southern part of the Loess Plateau, the headwaters of the Yellow River, and the eastern Tibetan Plateau. The daily rainfall is less than 0.5 mm d^{-1} in the Tarimu Basin, but greater than 7 mm d^{-1} in the southeast coastal region and even greater than 10 mm d^{-1} in part of the region (Fig. 7a). This summer rainfall pattern over China is well simulated by the RIEMS and RIEMS−AVIM model. The position of the isoline of the simulated daily rainfall of 3 mm d^{-1} is in accordance with the observed one. However, the simulated rainfall is deficient in parts of eastern China, but ex-

cessive in the Tibet Plateau and part of the Tianshan Mountains in comparison with the observed (Figs. 7b and 7c). The weaker western Pacific subtropical high and stronger Indian summer monsoon relative to the observed in the model atmosphere are responsible for the deviations of the above simulated summer rainfall. Much more moisture is transferred to the Tibetan Plateau, Northeast China and the area north of Northeast China, resulting in much more rainfall. The simulated rainfall of RIEMS-AVIM is less than that of RIEMS, and it is closer to the observed in most of China but less than that of RIEMS in the Sichuan Basin (Figs. 7b and 7c).

4. Simulation of sensible and latent heat fluxes

Energy and moisture exchanges are two major processes through which land surface affect climate change, and due to lack of reliable observation data, only the RIEMS and RIEMS-AVIM model simulated results are discussed here. Figures 8, 9, 10 and 11 give the distributions of simulated winter and summer sensible and latent heat fluxes over China, respectively.

Because temperature range between atmosphere and land surface is low and precipitation little in winter, the simulated surface sensible and latent heat fluxes are both small, with their values less than 10 W m^{-2} in most of northern China, and about 40 W m^{-2} in the south of South China. In summer, however, because of heating of radiation and increasing of precipitation, surface sensible and latent heat fluxes both distinctively increase, but with completely opposite distributive patterns, that is to say, there appears a west-high and east-low pattern in winter, while a reverse pattern in summer. The maximum value of sensible heat flux more than 120 W m^{-2} lies in the south of Tarimu Basin, and the minimum value less than 60 W m^{-2} in the east coastal area. The minimum value of summer latent heat flux less than 10 W m^{-2} is located in the desert region, and the maximum value more than 120 W m^{-2} in the coastal area of South China and the Yangtze River-Huaihe River Valleys. The simulated sensible and latent heat flux of RIEMS-AVIM are both less than the that of RIEMS in winter and summer, and the simulated sensible heat flux in eastern China and latent heat flux in Tibetan Plateau of RIEMS is obvious larger than the observed. In brief,

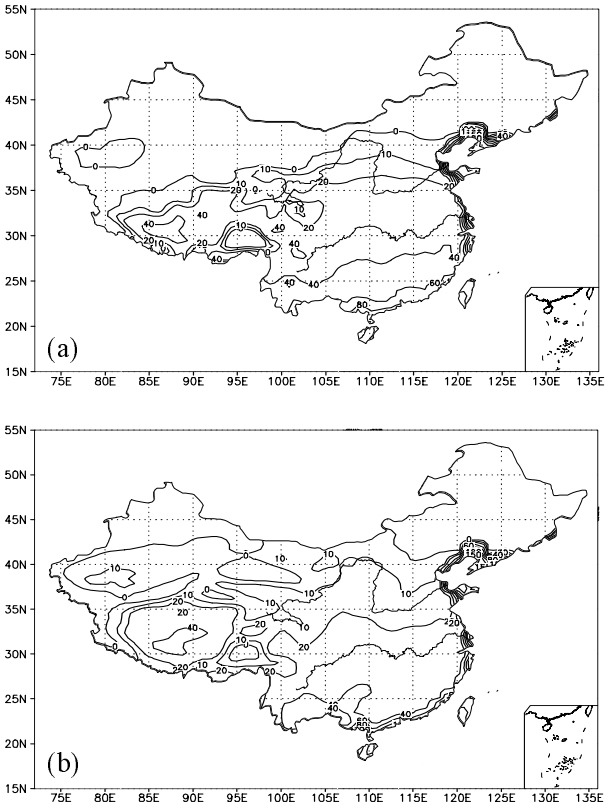

Fig. 8. (a) RIEMS and (b) RIEMS-AVIM simulated winter surface sensible heat fluxes (units: W m^{-2}).

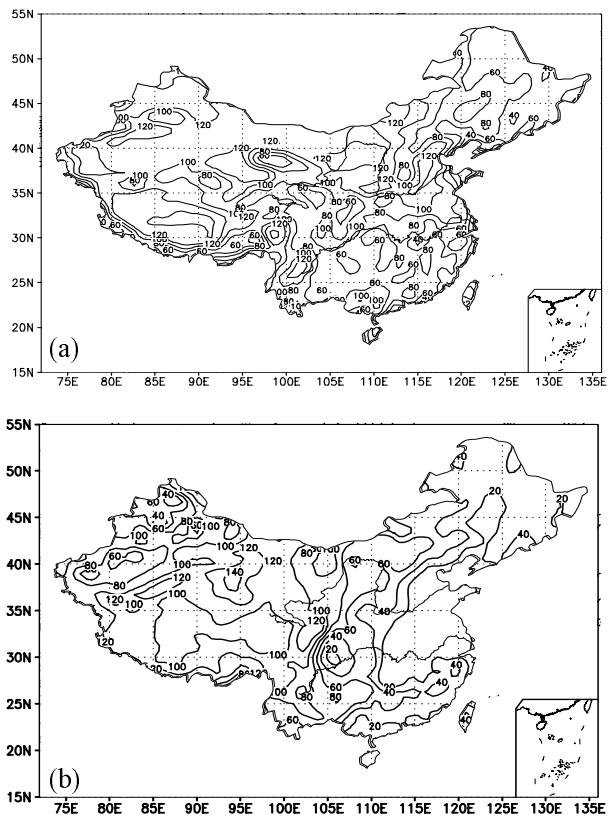

Fig. 9. (a) RIEMS and (b) RIEMS-AVIM simulated summer surface sensible heat fluxes (units: W m^{-2}).

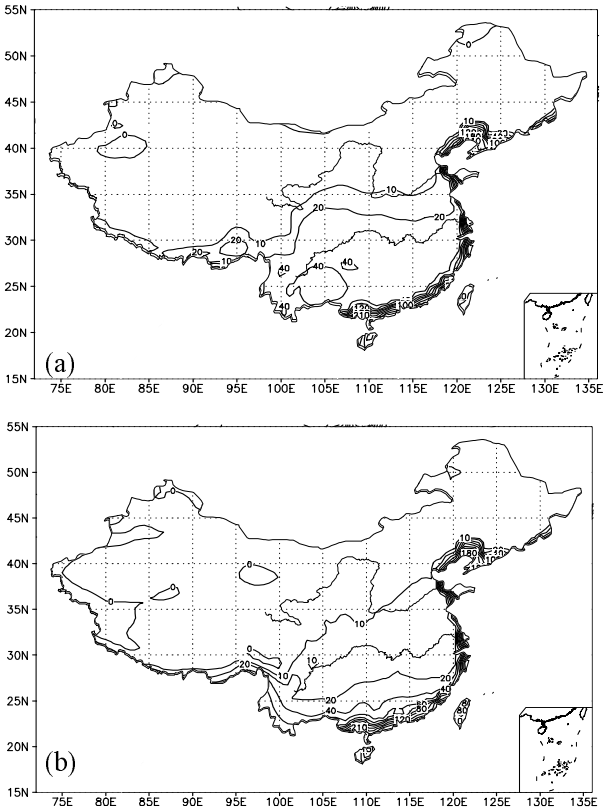

Fig. 10. (a) RIEMS and (b) RIEMS-AVIM simulated winter surface latent heat fluxes (units: W m^{-2}).

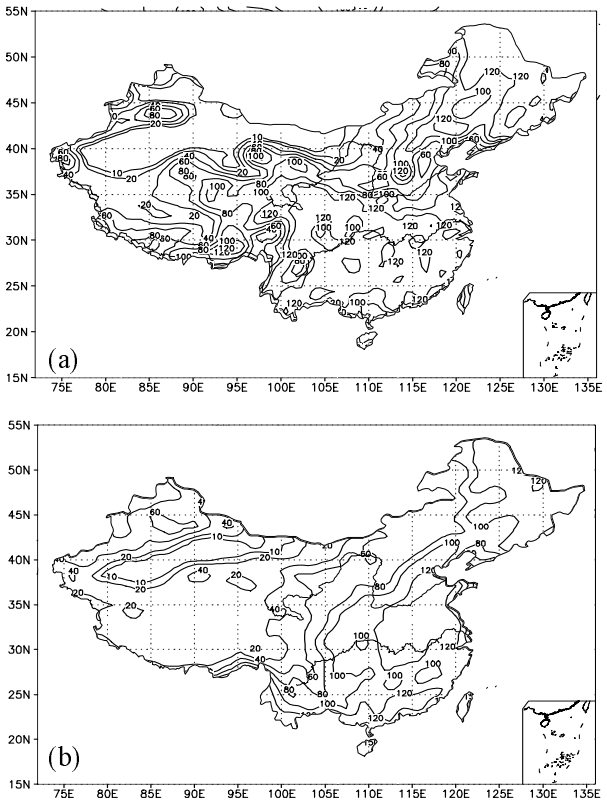

Fig. 11. (a) RIEMS and (b) RIEMS-AVIM simulated summer surface latent heat fluxes (units: W m^{-2}).

the above RIEMS-AVIM model simulated sensible and latent heat fluxes are basically in accord with their counterparts in "Climatological Atlas of the People's Republic of China" (Yan et al., 2002) in distributive patterns, but different to some extent in values. The lower sensible heat flux of RIEMS-AVIM in eastern China maybe result to the lower temperature bias between surface and air because of two-way coupling vegetation-atmosphere interaction, and the lower latent heat flux of RIEMS-AVIM in Tibetan Plateau is a result that more rainfall as runoff has been flowed away.

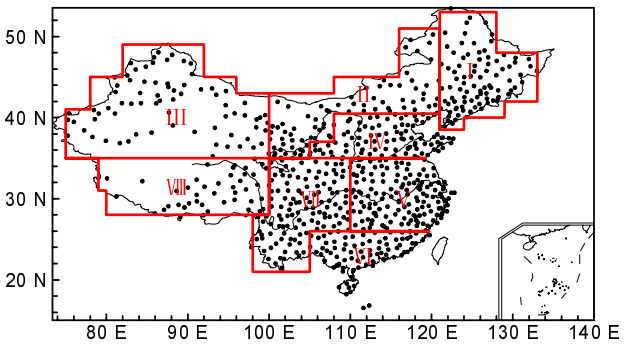

Fig. 12. The 740 meteorological stations distribution and climatic regions in China.

5. Seasonal and interannual variations of temperature and precipitation

China has a vast territory, and there are distinctively different geographic environments and climate in different areas. Eight climatic subregions [Fig. 12, Northeast China (NEC), Transition Region (TR), Northwest China (NWC), North China (NC), Central China (CC), South China (SC), Southwest China (SWC), and Tibetan Plateau (TP)] suggested by Zhang and Lin (1985) are used in this paper in testing the ability of climate simulation of RIEMS-AVIM model. Figures 13 and 14 show seasonal variations of temperature and precipitation in the eight climatic subregions. It can be seen from the two figures that the seasonal variations of temperature and precipitation in China are well simulated by the RIEMS and RIEMS-AVIM models, but are different to some extent in value. The simulated winter temperature is lower than the observed value, with the largest deviation in the Tibetan Plateau, the next in Southwest

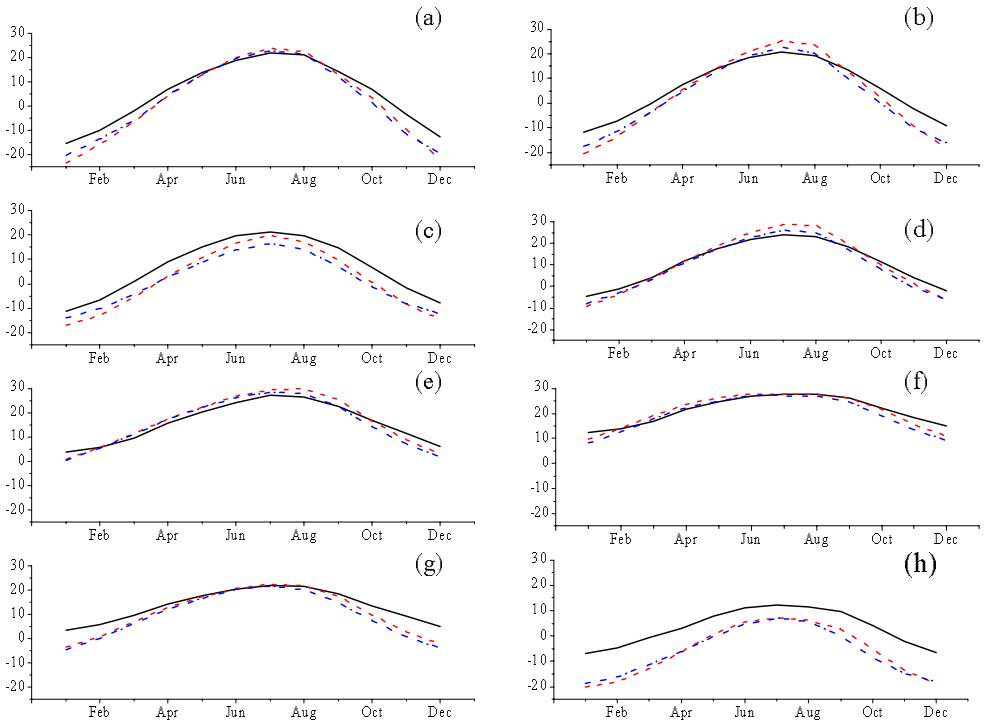

Fig. 13. Seasonal variations of observed (black solid line), RIEMS (red dashed line) and RIEMS-AVIM (blue dot and dashed line) simulated temperatures in eight subregions of China (units: °C; a, NEC; b, TR; c, NWC; d, NC; e, CC; f, SC; g, SWC; h, TP).

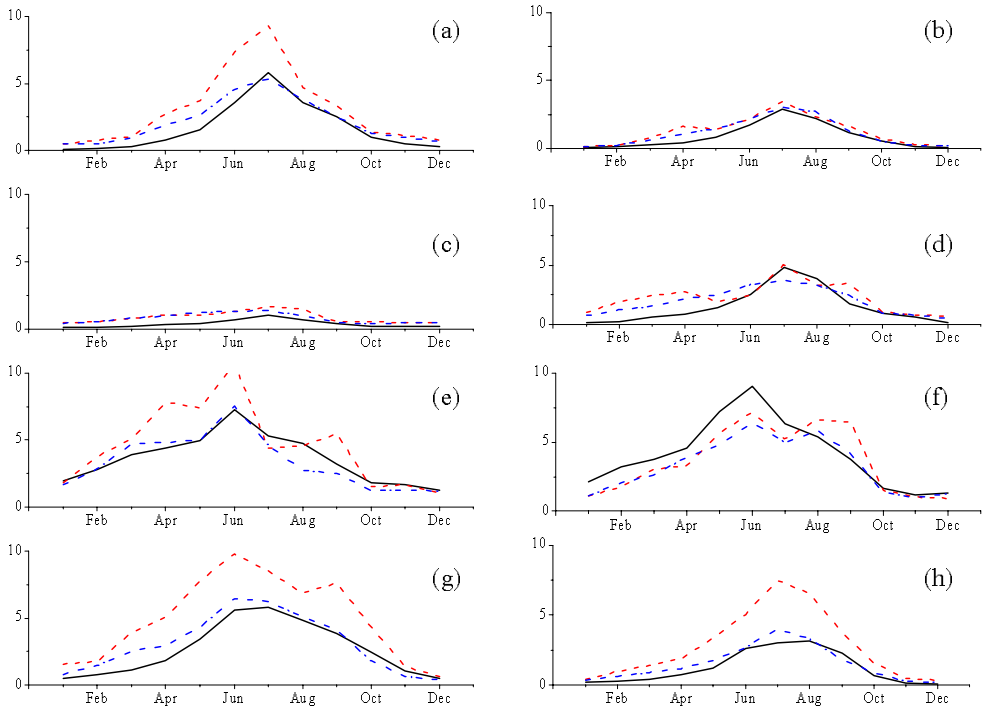

Fig. 14. Same as Fig. 13 but for monthly mean daily rainfall (units: mm d^{-1}).

Table 1. Correlation coefficients (r) between RIEMS-AVIM and RIEMS model simulated and observed temperatures for eight subregions.

Model	Area							
	NEC	TR	NWC	NC	CC	SC	SWC	TP
RIEMS	0.935*	0.896*	0.659*	0.684*	0.536	0.744*	0.052	0.499
RIEMS-AVIM	0.853*	0.650*	0.614	0.362	0.548	0.648*	0.107	0.675*

* shows that has passed significant level (α=0.05).

Table 2. Correlation coefficients (r) between RIEMS-AVIM and RIEMS model simulated and observed rainfall for eight subregions.

Model	Area							
	NEC	TR	NWC	NC	CC	SC	SWC	TP
RIEMS	0.590	0.545	0.661*	−0.001	−0.153	0.355	−0.856*	−0.314
RIEMS-AVIM	0.413	0.370	0.690*	0.410	0.559	0.498	−0.329	−0.135

* shows that has passed significant level (α=0.05).

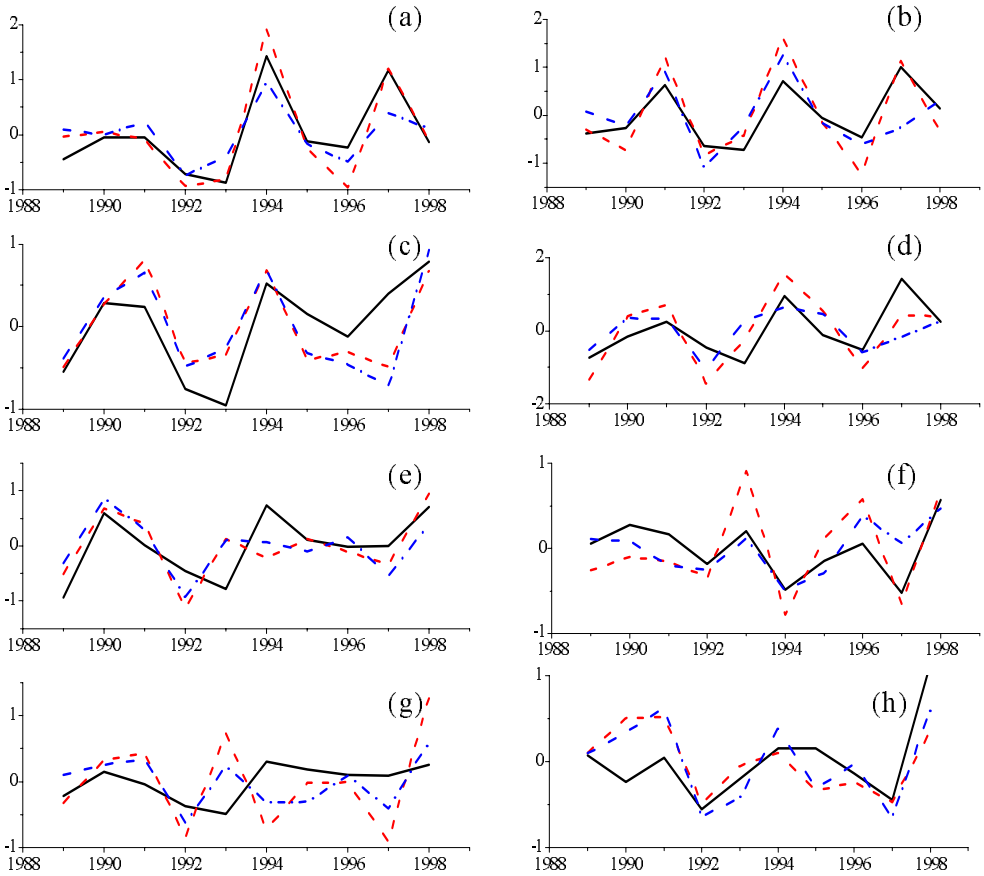

Fig. 15. Interannual variations of observed (black solid line), RIEMS (red dashed line) and RIEMS-AVIM (blue dot and dashed line) simulated temperatures in eight subregions of China(units: °C ; a, NEC; b, TR; c, NWC; d, NC; e, CC; f, SC; g, SWC; h, TP).

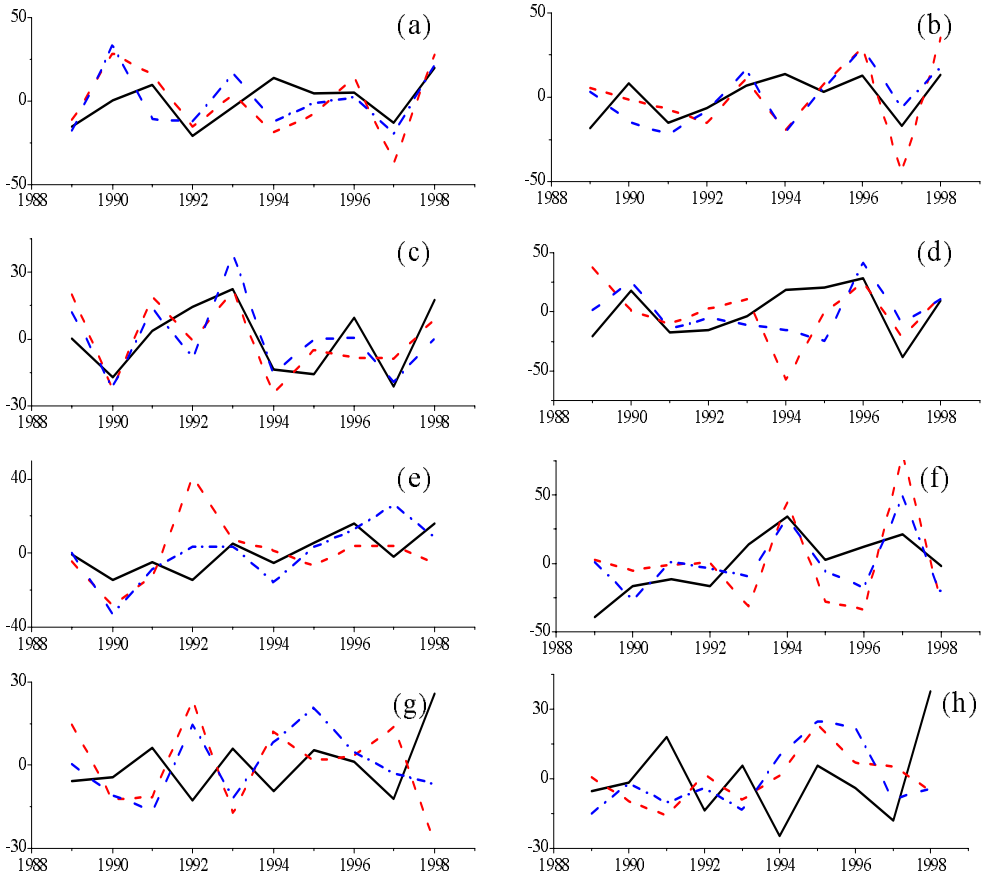

Fig. 16. Same as Fig. 15 but for interannual variations of summer rainfall anomaly (units: mm d^{-1}).

China, and a deviation of about 2°C–4°C in other subregions; while the simulated summer temperature is basically in accordance with the observed value in eastern China, but lower by about 1°C–3°C in western China. The simulated temperature of RIEMS-AVIM is higher in winter and lower in summer than that of RIEMS, which shows that the simulated temperature of RIEMS-AVIM is closer to the observed value. The lower annual range of air temperature of RIEMS-AVIM maybe result to the variational vegetation. The simulated rainfall is more than the observed in the first half of the year in most subregions except for South China, and is in accordance with the observed in the second half year. The simulated rainfall of RIEMS-AVIM is closer to that of RIEMS in most of China. We believe that the improvement of RIEMS-AVIM regarding rainfall may be a result of the lower sensible heat flux in eastern China and lower latent heat flux in the Tibetan Plateau, which makes the ascending motion weaken.

Figures 15 and 16 display the interannual variations of summer temperature and rainfall anomalies in the eight subregions. It is shown in the two figures that the general simulated interannual trend of temperature and precipitation increase is basically in agreement with the observed one, but there are larger deviations of year-by-year interannual variations between the simulation and observation. On the whole, the simulation of interannual variation for temperature is better than that for precipitation. In the 10 years, the simulated temperature matches well with the observed temperature in most years in seven subregions except for Southwest China (Fig. 15), and their correlations are significant at a α=0.05 significant level in Northeast China, Transition Region, South China and the Tibetan Plateau. The correlation coefficients are also relatively high in Northwest China and Central China (Table 1). The simulated rainfall anomaly does not match very well with the observed year-by-year since the simulated precipitation anomalies are frequently opposite of the observed in Southwest China and the Tibetan Plateau. In the other six subregions it matches well only in five out of the ten years. The correlation between RIEMS-AVIM and observation is sig-

nificant at the α=0.05 significant level only in Northwest China, and RIEMS only in Northwest China with a significant negative correlation in Southwest China.

6. Conclusions

It has been found from the above analyses that the RIEMS-AVIM model has fair ability for climate simulation in China, and after further improvement it could be used in a simulation study on regional-scale interaction between air and vegetation. Main conclusions are as follows:

(1) The RIEMS-AVIM model is able to simulate spatial distributive characteristics of regional temperature and precipitation over China fairly well; however, the values of temperature and rainfall are under-simulated in some subregions, such as the Tibetan Plateau, and oversimulated in other subregions. The summer rainfall is under-simulated in subregions in eastern China, but oversimulated in the Tibetan Plateau and part of the Tianshan Mountains.

(2) Distributions of RIEMS-AVIM simulated ground surface sensible and latent heat fluxes are consistent with actual patterns (climatological atlas), i.e., both sensible and latent heat fluxes are lower over the whole country in winter, and in summer the sensible heat flux shows a pattern of west-high-east-low, while the latent heat flux displays a pattern of east-high-west-low.

(3) Seasonal variations of simulated temperature and precipitation of RIEMS-AVIM are in accordance with those of the observed. Temperature is under-simulated over both the Tibetan Plateau and Northwest China for the whole year, while in other subregions it is slightly under-simulated in winter, but in agreement with the observed in summer. The simulated temperature of RIEMS-AVIM is higher in winter and lower in summer than that of RIEMS, which shows that the simulated temperature of RIEMS-AVIM is closer to the observed value. Simulated precipitation is excessive in the first half of the year, but consistent with the observed in the second half of the year. The simulated summer precipitation of RIEMS-AVIM has significant improvement compared to that of RIEMS, which is less, and closer to the observed value.

(4) The RIEMS-AVIM model is also able to simulate the interannual variations of temperature and precipitation fairy well, and temperature simulation is better than rainfall simulation. The interannual variations of simulated temperature are significantly correlated with the observed in Northeast China, Transition Region, South China, and the Tibetan Plateau, however, the correlation of interannual variations for rainfall between simulation and observation is only significant in Northwest China.

Acknowledgements. The authors would like to thank Profs. Ji Jinjun and Feng Guolin, Drs. Dan Li and Feng Jinmin, and the anonymous reviewers for their comments and suggestions. This research was supported by the National Basic Research Program of China from the Ministry of Science and Technology of China (Grant No. 2006CB400500 and 2007CB411505) and the National Natural Science Foundation of China (Grant No. 40705031)

REFERENCES

Chen, M., and D. Pollarid, 2004: Development and application of an interactive climate-ecosystem model system. *Chinese Science Bulletin*, **48**(Supp. II), 44–55.

Chen, M., D. Pollarid, and E. J. Barron, 2004: Regional climate change in East Asia simulated by an interactive atmosphere-soil-vegetation model. *J. Climate*, **17**, 557–572.

Cox, P. M., R. A. Betts, C. D. Jones, S. A. Spall, and L. J. Totterdell, 2000: Acceleration of global warming due to carbon-cycle feedbacks in a coupled climate model. *Nature*, **408**, 184–187.

Dan, L., J. J. Ji, and Y. P. Li, 2005: Climatic and biological simulations in a two-way coupled atmospherie-biosphere model (CABM). *Global and Planetary Change*, **47**, 153–169.

Feng, J. M., 2006: Comparative study on the ten-year integration of various regional climate models for Asia, Ph. D. dissertation, Chinese Academy of Sciences, 223pp. (in Chinese)

Foley, J. A., S. Levis, I. C. Prentice, D. Pollard, and S. L. Thompson, 1998: Coupling dynamic models of climate and vegetation. *Global Change Biology*, **4**, 561–579.

Fu, C. B., H. L. Wei, and Y. Qian, 2000: Documentation on a regional integrated environment model system(RIEMS version 1), TEACOM Science Report No.1, START Regional Committee for Temperate East Asia, Beijing, China, 26pp.

Fu, C. B., and Coauthors, 2005: Regional climate model intercomparison project for Asia. *Bull. Amer. Meteor. Soc.*, **86**, 257–266.

Ji, J. J., 1995: A climate-vegetation interaction model, simulating physical and biological processes at the surface. *Journal of Biogeography*, **22**, 445–451.

Ji, J. J., and Y. C. Hu, 1989: A simple land surface process model for use in climate studies. *Acta Meteorologica Sinica*, **3**, 342–351.

Lu, L. X., R. A. Pielke, G. E. Liston, W. J. Parton, D. Ojima, and M. Hartman, 2001: Implementation of a two-way interactive atmospheric and ecological model and its application to the central United States. *J. Climate*, **14**, 900–919.

Nemani, R. R., C. D. Keeling, H. Hashimoto, W. M. Jolly, S. C. Piper, C. J. Tucker, R. B. Myneni, and S. W.

Running, 2003: Climate-Driven Increases in Global Terrestrial Net Primary Production from 1982 to 1999. *Science*, **300**, 560–1563.

Snyder, P. K., J. A. Foley, M. H. Hitchman, and C. Delire, 2004: Analyzing the effecs of complete tropical forest removal on the regional climate using a detailed three-dimensional energy budget, a application to Africa. *J. Geophys. Res.*, **109**, D21102, doi: 10.1029/2003JD004462.

Song, S., C. B. Fu, L. Zhou, and H. J. Wang, 2003: Two-way coupling experiment of REGCM2 and SUCROS models. *Acta Meteorologica Sinica*, **61**(6), 702–711. (in Chinese)

Tsvetsinskaya, E. A., L. O. Mearns, and W. E. Easterling, 2001: Investigating the effect of seasonal plant growth and development in 3-dimensional atmospheric simulations: Part II: atmospheric response to crop growth and development. *J. Climate*, **14**, 910–729.

Yan, H., and Coauthors, 2002: Climatological Atlas of the People's Republic of China, China Meteorological Press, 250pp.

Zhang J. C., and Z. G. Lin., 1985: *Climate in China*. Shanghai Science Technology Press, Shanghai, 467–505.

Zhang, J. Y., 2005: Effects of changes in land cover/land use on regional climate. Ph. D dissertation, Chinese Academy of Sciences, 120pp. (in Chinese)

Zeng, N., J. D. Neelin, K. M. Lau, and C. J. Tucker, 1999: Enhancement of interdecadal climate variability in the Sahel by vegetation interaction. *Science*, **286**, 1537–1540.